

Article ID: 1006-8775(2000) 02-0113-10

PRELIMINARY ANALYSES OF THE ACTIVITIES OF SOUTH CHINA SEA SUMMER MONSOON IN 1998

LIANG Jian-yin (梁建茵) and WU Shang-sen (吴尚森)

(Guangzhou Institute of Tropical and Oceanic Meteorology, Guangzhou, 510080 China)

ABSTRACT: The NCEP reanalyzed data, OLR and SST observations are used to study the onset time and the multi-time scales features of the South China Sea (SCS) summer monsoon in 1998 and its interaction with the sea surface temperature and the effect on the precipitation in Guangdong province. It is found that the 1998 SCS summer monsoon set in on May 17 (in the fourth pentad of the month). The year witnesses a weak monsoon with the OLR oscillating at cycles of about 1 month and the Southwest Monsoon of about 1/2 month. The monsoon over the Bay of Bengal and the cross-equatorial current near 105° are two driving forces for low-frequency variations of the SCS monsoon. The weak activity in the year was resulted from positive anomalies of SST in the equatorial eastern Pacific in early spring and subsequent formation of positive anomalies of SST in the SCS through the Arabian Sea.

Key words: South China Sea; Southwest Monsoon; analysis

CLC number: P425.42 **Document code:** A

1 INTRODUCTION

As shown in studies on East Asian monsoons in recent years (Ding and Ma, 1996), the SCS monsoon breaks out on the earliest date among monsoon systems in Asia, averaging in the middle decade of May. It then transports westward to India and northward to eastern China, Japan and the Korean Peninsula. Apart from studies with OLR and TBB data (Chen, Song and Murakami, 1996; He and Luo, 1996; Liu, Xie and Ye, 1998), Lau and Song (1997) study pentad and monthly mean data concerning global precipitation, winds, and geopotential heights for 1986 ~ 1994 (9 years). With data of 10 years or more recorded at stations on islands and coast (Yan, 1997), analysis of pentad-mean ECMWF wind fields and OLR data for 30 years (1959 ~ 1988) (Wang, 1997), and study on 30 years (1959 ~ 1988) of conventional surface observations and 9 years of rawinsonde observations on the Xisha Islands in the northern SCS (Wu and Liang, 1998), we know that the averaged date of onset of the Southwest Monsoon is in the middle decade of May in the SCS.

Changes in the intensity of the summer monsoon are much dependant on those in the SST of the tropical ocean. Comparing and studying years of strong and weak Asian summer monsoons, Li and Michio (1996) point out that for the years of strong (weak) monsoon there is negative (positive) SSTA over the equatorial eastern Pacific, Arabian Sea, Bay of Bengal and SCS while there is positive (negative) SSTA in the equatorial western Pacific. Webster and Yang (1992) suggest a

Received date: 1999-10-13; **revised date:** 2000-09-15

Foundation item: Scaling Project A of the Ministry of Science and Technology "the research on South China Sea Monsoon Experiments" and Foundation of Meteorological Science for Young Scientists by the China Meteorological Administration

Biography: LIANG Jian-yin (1964 -), male, native from Shunde City Guangdong Province, high-ranking researcher at Guangzhou Institute of Tropical and Oceanic Meteorology, holder of Master Degree, undertaking the study of climatology.

"selective interaction" between the Asian summer monsoon and ENSO after addressing the variation of the former and its relation with the latter. Wu and Meng (1998) argue that the anomalies of the zonal circulation over the Indian Ocean, through gear-like coupling between atmospheric systems for the Indian Ocean and Pacific Ocean, govern the air-sea interactions in the equatorial eastern Pacific and set off the ENSO episode.

It is the main purpose of the current work that a Southwest Monsoon index is used to diagnose the set-up of the SCS Southwest Monsoon and multi-time-scale variations of the intensity and a study is conducted of the coupling relation between the SST variation in the equatorial Pacific, SCS, and tropical Indian Ocean and the monsoon variation in the SCS region.

2 DATA PROCESSING AND SCS SOUTHWEST MONSOON INDEX

The paper uses the NCEP reanalyzed fields and OLR data that have a resolution of $2.5^\circ \times 2.5^\circ$ and cover a period from 1979 to 1998. The data are the weekly $1^\circ \times 1^\circ$ SST provided by NCEP that extend from 1982 to 1998. The data have been interpolated linearly to be based on pentad.

The index (Liang, Wu and You, 1999) for the Southwest Monsoon, which combines the southwesterly component and OLR, is expressed by

$$I_{\text{SCSMS}} = (V_{\text{SW}} - 1.0) / a + (235.0 - V_{\text{OLR}}) / b$$

For the expression, I_{SCSMS} is the index for the Southwest Monsoon, V_{SW} is the wind speed of the southwesterly component (unit in m/s), and V_{OLR} is the OLR (unit in W/m^2). Both V_{SW} and V_{OLR} are the pentad mean for the region ($5^\circ\text{N} \sim 20^\circ\text{N}$, $105^\circ\text{E} \sim 120^\circ\text{E}$) in the SCS. The constants adopt their values based on thresholds of greater than 1.0 m/s for the southwesterly component and less than $235.0 \text{ W}/\text{m}^2$ for the OLR. As regard to a and b , they are respectively half of the standard deviations of the pentad component of the southwesterly and pentad OLR in June ~ August, specifically $a = 1 \text{ m/s}$ and $b = 10 \text{ W}/\text{m}^2$, in rough magnitude.

3 ESTABLISHMENT OF SCS SOUTHWEST MONSOON IN 1998

The Southwest Monsoon is defined to set up in the SCS when the monsoon index grows above zero for the first time ever in relevant computations. Fig.1 gives the day-to-day variation curves of the monsoon index in 1998, which indicates the onset date to be May 17 (in the fourth pentad of May) for the Southwest Monsoon in the SCS. For the same index, the monsoon establishment is also determined to be in the fourth pentad of May from 1979 to 1995, computing

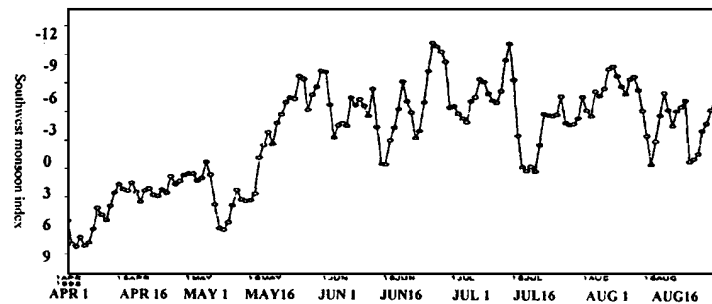


Fig.1 The curve of the daily summer monsoon index of 1998.

pentad-based mean. It is seen that the 1998 monsoon falls within the normal range of establishment.

Identical conclusions can also be reached using the component of the southwesterly and the OLR profiles. Fig.2a is a cross section (treated with 5-day running mean, same below) over time in terms of day-to-day OLR variations averaged over $105^{\circ}\text{E} \sim 120^{\circ}\text{E}$ from April to August in 1998. It is known that zones of major convection are active south of the equator for April and the time before May 16; convection grows explosively in the northern SCS and South China region on May 17 before extending southward steadily. Examining the pentad-based time cross section of OLR averaged over $5^{\circ}\text{N} \sim 20^{\circ}\text{N}$ April through August in 1998 (Fig.2b), intense convection takes place near $70^{\circ}\text{E} \sim 80^{\circ}\text{E}$ as early as May 10 and gradually transfers from east to west and the SCS region begins to have such development on May 17.

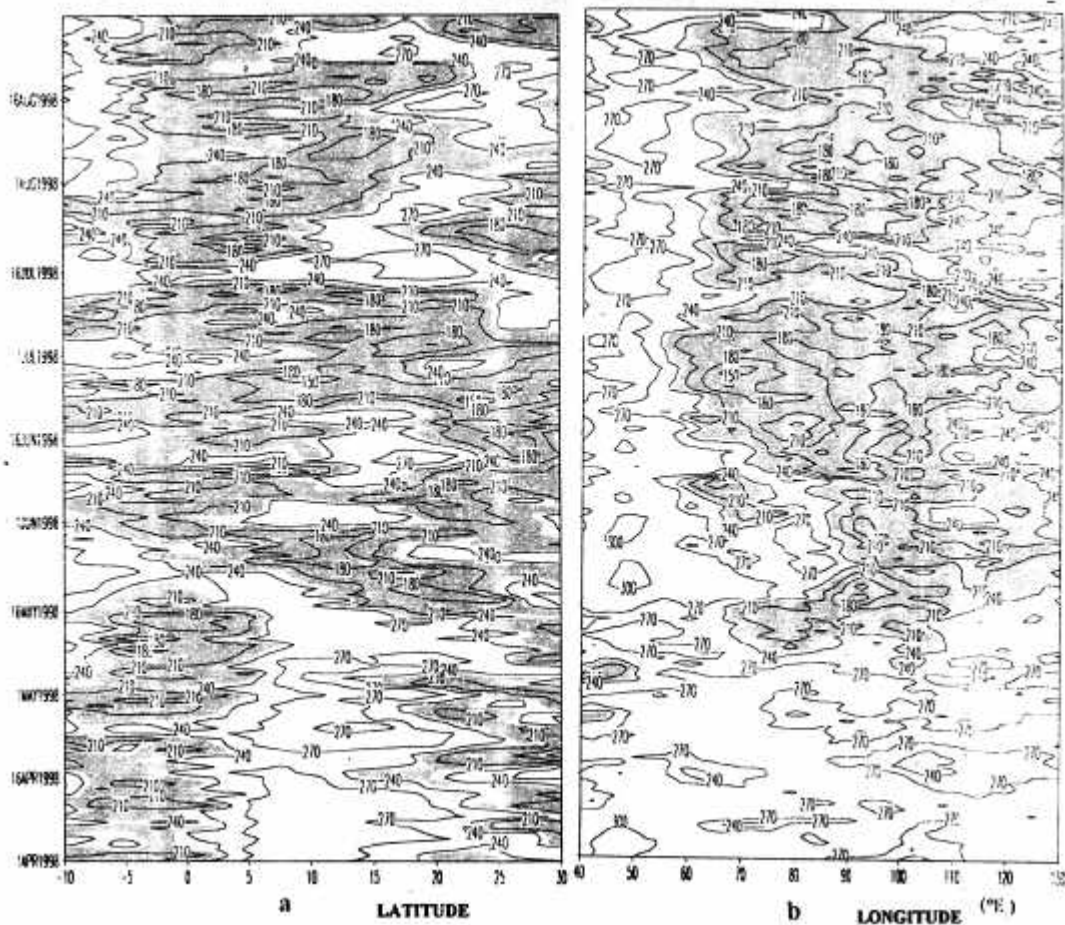


Fig.2 The time cross section of 5-day running mean OLR averaged within $105^{\circ}\text{E} \sim 120^{\circ}\text{E}$ (a) and $5^{\circ}\text{N} \sim 20^{\circ}\text{N}$ (b); shaded region for OLR less than 230 W/m^2

The time-latitude cross section for day-to-day variation of the 850-hPa southwesterly component is given in Fig.3 that has been averaged over $105^{\circ}\text{E} \sim 120^{\circ}\text{E}$ from April to August 1998. It is clear that the southwesterly has occurred in April over the continent of China with high-value zones of wind speed over the south of China. It is jointly caused by the southern branch of the westerly trough in mid-latitudes and the southwesterly flow to the northwest of the subtropical high, rather than the tropical southwest monsoon (northeasterly before mid-May in areas south of

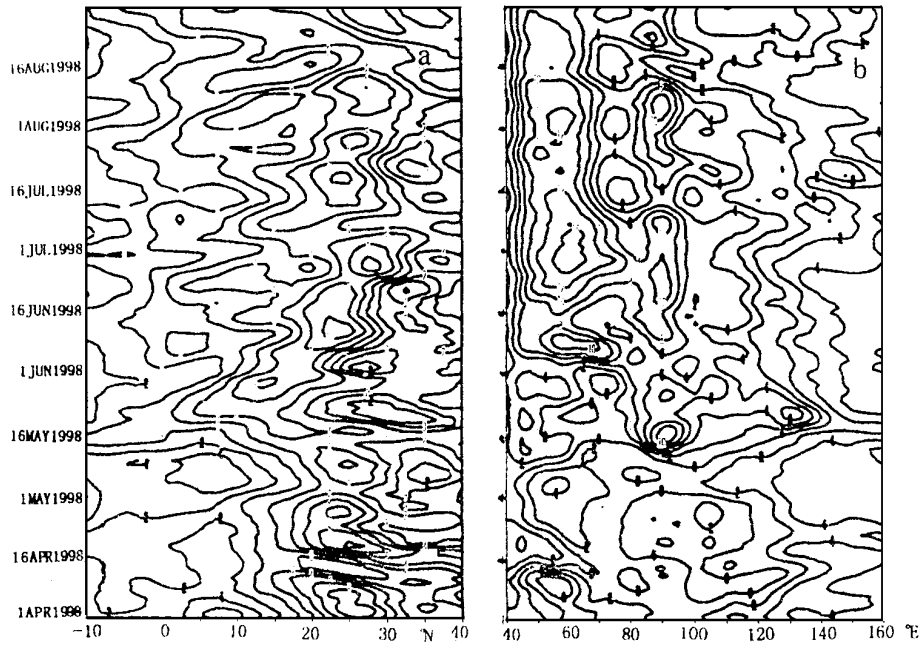


Fig.3 The time cross section of daily SW wind component averaged for 105°E ~ 120°E (a) and 5°N ~ 20°N (b)

16°N). The southwesterly wind spreads all over the latitudes 0° ~ 20°N on May 17. From April to August 1998, day-to-day southwesterly components averaged over 5°N ~ 20°N indicate, in the time cross section, that a strong southwesterly component (>4m/s) first (in the third pentad of May) appears near 90°E (i.e. the region of the Bay of Bengal) and subsequently the southwesterly rapidly spreads from west to east to affect the SCS and western part of Pacific Ocean.

Fig.4 is the composite chart combining the third pentad of May (one pentad before the out-

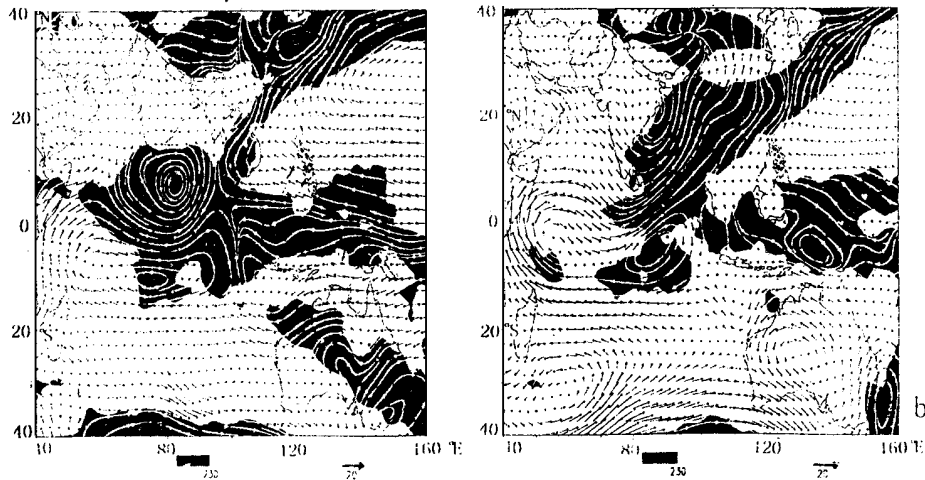


Fig.4 Composite chart of 850-hPa flow field and OLR before (a) and in (b) the pentad of SW monsoon set-up in the SCS; shaded region for OLR less than 230 W/m²

break) and the fourth pentad of May (the very pentad when the outbreak takes place) with respect to the SCS Southwest Monsoon. In the third pentad of May, the tropical convergence is located over the tropical Indian Ocean, western Pacific and around the equator so that most of the SCS region is controlled by the subtropical high. Intense convection north of the subtropical high is a combined result of cold air activity from the northern parts of China and the southwesterly flow deviating from the high. In the fourth pentad of May, the tropical convergence makes a large shift to the north with much more obvious reflection in the SCS region where convection develops vigorously. Consequently, the subtropical high moves out of the SCS, leaving the southwesterly there in the control of strong southwesterly from the Bay of Bengal and the cross-equatorial air current near 105°E , highlighting the characteristics of the Southwest Monsoon.

A consistent conclusion can be reached from the analysis above that the SCS Southwest Monsoon sets up on May 17 in 1998.

4 VARIATION OF SOUTHWEST MONSOON INTENSITY IN SCS

Take $I_{\text{SCSMS}} > 0$ as the period with the Southwest Monsoon prevalence and $I_{\text{SCSMS}} = 0$ as the one without it. By removing seasonal signals from the series anomaly, the value is shown as zero during the southwest-monsoon free period. The treatment performs well in revealing anomalous changes of the monsoon. Employing the wavelet analysis technique of MHAT, we add to the treatment a time scale parameter $a = 9 \times 2^{j-1}$, with $j = 0, 1, 2, 3, 4$, and 5.

Apply the MHAT wavelet analysis to the anomaly series of the Southwest Monsoon. Fig.5 presents the results of the analysis on various time scales. Specifically, $a = 9$ is equivalent to the seasonal time scale, $a = 36$ to the inter-annual time scale, and $a = 144$ equivalent to the multi-year time scale.

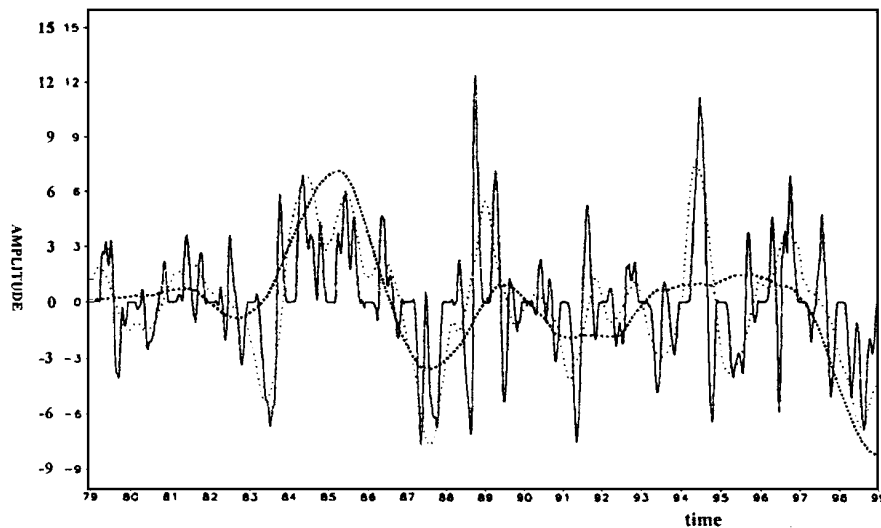


Fig.5 MHAT wavelet-transformed curves for the SCS summer monsoon index; solid line for $a = 9$, dashed line for $a = 36$, dotted line for $a = 144$

For the inter-annual scale (dashed line), years of strong monsoons are in 1981, 1984, 1985, 1986, 1994, and 1996 and years of weak monsoons are in 1983, 1987, 1991, 1993, 1995, and 1998,

when peak values larger than 2 (smaller than -2) between May and September are defined as strong (weak) monsoon years. The years 1979, 1980, 1982, 1990, 1992, and 1997 are in the normal range. The years 1988 and 1989 are relatively peculiar, with the former being weak during the first half of the Southwest Monsoon but stronger in the latter half and the otherwise is true for 1989. It can be seen that 1998 is one of the years that witness weak Southwest Monsoon.

Let's look at the oscillations of the OLR in the SCS region and the southwesterly component during the summer monsoon in 1998. Fig.6 is the distributions of wavelet transformation for

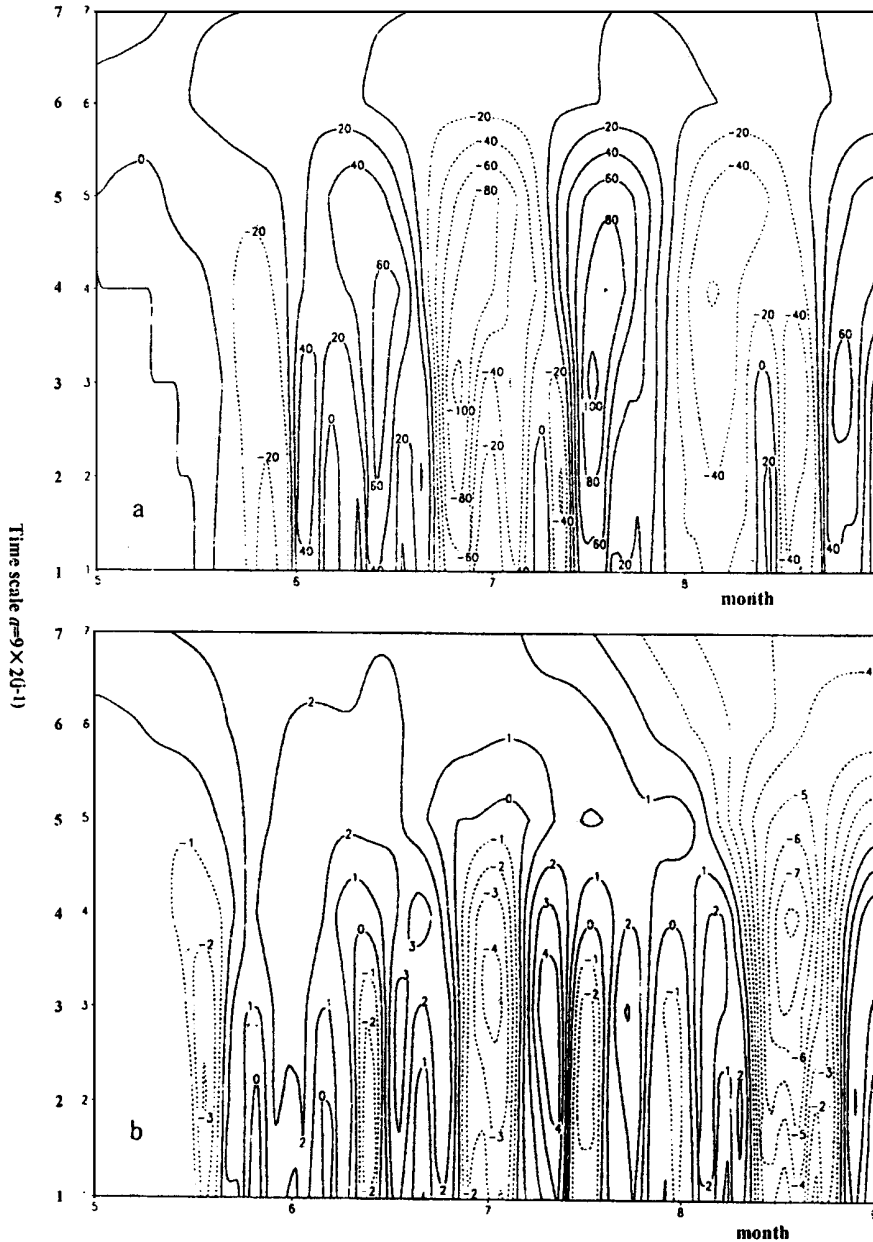


Fig.6 Distributions of wavelet transformation for daily OLR (a) and SW wind component (b); shaded region for positive values

day-to-day OLR and southwesterly components, averaged over the SCS region from May to August 1998. Fig.6a clearly depicts the low-frequency oscillations of OLR with cycles of about 1 month during the period. High-value periods (weak convection) center around mid-June, mid-July, and late August while low-value periods (strong convection) around late May, late June, and early August. It can be known that obvious differences exist between OLR and the southwesterly wind concerning the cycles of oscillation, with loose relationship between the OLR in the SCS and the local southwesterly wind in terms of oscillatory variation.

In contrast, the relation is quite significant between the OLR in the SCS and the southwesterly component in the Bay of Bengal, with correlation coefficient being -0.57 . Fig.7a gives the cross section of the component varying with time on a daily basis averaged over $5^{\circ}\text{N} \sim 20^{\circ}\text{N}$ 1998. For Fig.7a, large values of the southwesterly wind appear near 90°E (region of the Bay of Bengal) and 60°E , intervening with zones of relatively small values between 70°E and 80°E . It indicates that there is a sharp decrease of the Southwest Monsoon when passing over the Indochina Peninsula, weakening the effects of the Indian Monsoon on the monsoon over the Bay of Bengal. The southwesterly component near the 90°E is featured by well-defined low-frequency variation that oscillates at about a month. The peaks occur in the mid- and late-May, late June, and late July through early August, being consistent with the low values of OLR in the SCS. Although the southwesterly wind in the SCS region seems not to relate closely to that in the region of Bay of Bengal, increased southwesterly wind in the former is always associated with similar trends of that for the latter. Therefore, it is safe to state that the Bay of Bengal region is one of the driving forces for the low-frequency oscillations in the SCS monsoon.

In addition, the cross-equatorial flows are also playing an important role. Fig.7b gives the time

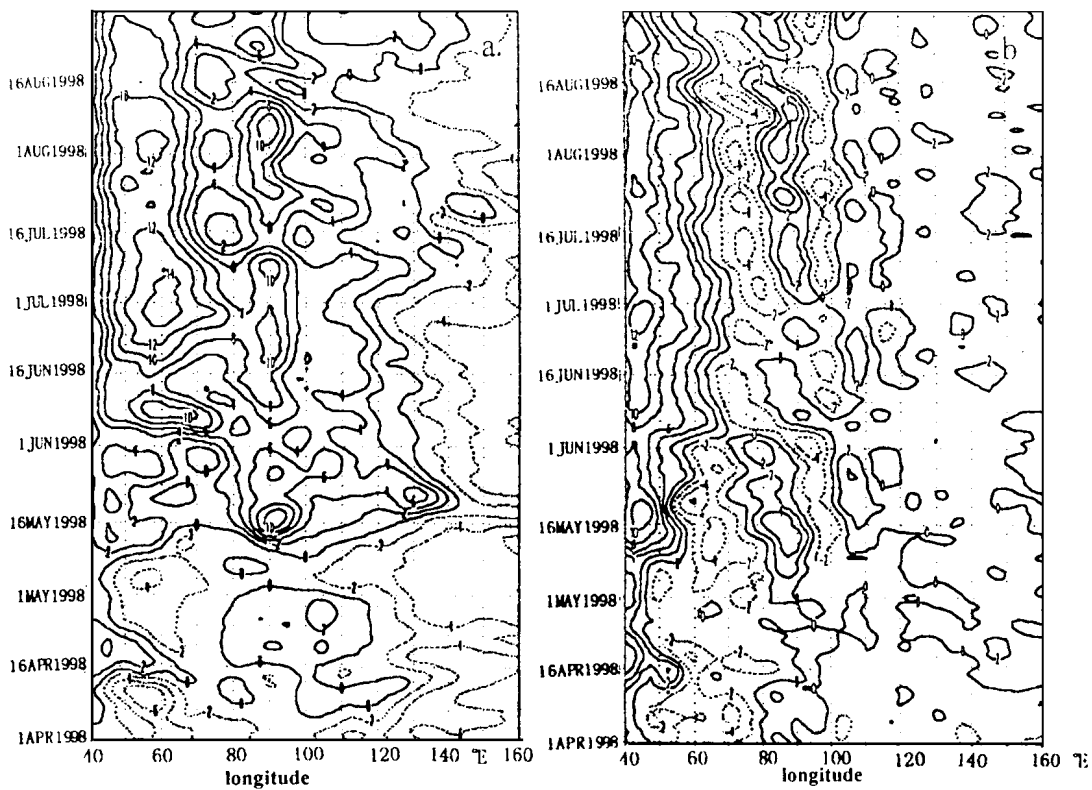


Fig.7 Time cross section of 5-day running mean SW wind component averaged for $5^{\circ}\text{N} \sim 20^{\circ}\text{N}$ (a) and v component averaged for $5^{\circ}\text{S} \sim 5^{\circ}\text{N}$ (b)

cross sections day-to-day north and south wind components that are averaged over $5^{\circ}\text{S} \sim 5^{\circ}\text{N}$ in 1998. As they are shown in the figure, three strong cross-equatorial air currents, the most northern of which being between $40^{\circ}\text{N} \sim 50^{\circ}\text{N}$, not only affect the variation of the Indian summer monsoon, but corresponds to some extent to the changes in the southwesterly in the Bay of Bengal. Examples are the appearance of peaks in the mid- and late-May and late June. Another air-flow crossing the equator appears between $80^{\circ}\text{E} \sim 90^{\circ}\text{E}$ with peaks in the mid- and late-May and late July through early August. The third flow occurs near 105°E , varying with clear low-frequency characteristics (at cycles of about half a month) in terms of intensity and oscillating almost simultaneously with the half-month cycles found in the southwesterly wind in the SCS region.

Summarizing the work above, we have come to the conclusions below. For the duration of summer monsoon, the southwesterly wind in the SCS region is marked by low-frequency oscillations at cycles of about half a month, which is caused mainly by the cross-equatorial current near 105°E . The OLR is featured by oscillations of about 1 month, which is mainly resulted from the southwesterly from the Bay of Bengal.

5 SOUTHWEST MONSOON IN SCS AND COUPLING WITH SST

To study the relationship between the variation of SSTA and Southwest Monsoon, wavelet analysis is done of the SCS ($5^{\circ}\text{N} \sim 20^{\circ}\text{N}$, $105^{\circ}\text{E} \sim 120^{\circ}\text{E}$), the Arabian Sea ($5^{\circ}\text{N} \sim 20^{\circ}\text{N}$, $50^{\circ}\text{E} \sim 70^{\circ}\text{E}$), the equatorial eastern Pacific ($0^{\circ} \sim 10^{\circ}\text{N}$, $180^{\circ} \sim 90^{\circ}\text{W}$), and the west Pacific ($5^{\circ}\text{N} \sim 20^{\circ}\text{N}$, $140^{\circ}\text{E} \sim 160^{\circ}\text{E}$) in terms of pentad-to-pentad SSTA. The results are then compared with the wavelet-transformed index anomalies of the Southwest Monsoon. Tab.1 shows the maximum correlation coefficient and lagging time in various time sequences for Southwest Monsoon index (MHAT) and wavelet-transformed series of SST in various areas of the ocean. The negative value indicates that the variation of SST is lagging behind that of the Southwest Monsoon index.

Tab.1 Maximum correlation coefficient and lagging time in various time sequences between Southwest Monsoon index (I_{SCSMS}) and MHAT wavelet transform of SST series in various parts of the ocean

Time scale	item	SCS	Arabian Sea	Equatorial W.P.	Equatorial E.P.
Multi-yr	Max. Time coef.	-0.66	-0.83	0.21	-0.45
	Lagging time (pent.)	-8	-6	-7	-7
Inter-yr	Max. Time coef.	-0.54	-0.78	0.52	-0.63
	Lagging time (pent.)	-18	-19	13	12
Seasonal	Max. Time coef.	-0.32	-0.46	0.35	-0.37
	Lagging time (pent.)	-11	-12	4	26

The intensity of the Southwest Monsoon is significantly in negative correlation with the SSTA in the equatorial eastern Pacific but in positive correlation with that in the western Pacific. It shows that the Southwest Monsoon variation acts passively in the interactions between ENSO and the SCS southwest monsoon, particularly so on the inter-annual time scale. It is statistically shown that the equatorial eastern Pacific is of negative (positive) anomaly in early spring of strong (weak) monsoon years (the latter with the exception of 1991). An illustration is that a positive anomaly in the equatorial eastern Pacific in early spring of 1998 corresponds to a weak monsoon year for the SCS. It suggests that the ENSO is an important factor in affecting the inter-annual variation of the SCS southwest monsoon.

On all time scales, especially the multi-year scale, the Southwest Monsoon shows a significant

negative correlation earlier than the variation of SSTA in the SCS through the Arabian Sea. It is sign that the SCS Southwest Monsoon (and the Asian summer monsoon in a broader sense) plays an active role in its interactions with the SST of these waters — a strong (weak) southwesterly lead to decreased (increased) SST in the subsequent period.

The year 1998 having a strong El Niño, the southwest monsoon in the SCS is obviously weakened in the SCS, resulting in higher SST in the SCS through the Arabian Sea. The year is typical in reflecting the effects of the SCS monsoon on the SST in the SCS-Arabian-Sea region.

6 CONCLUDING REMARKS

The following points are what we have learned from the study above with respect to the set-up and variation of the Southwest Monsoon in the South China Sea. All studies, whether done from the monsoon index, the southwesterly wind component in the SCS, time cross section for the OLR or from the 850-hPa circulation and OLR composite charts before and after the monsoon setting-up, indicate that the 1998 SCS Southwest Monsoon set up on May 17. The southwesterly wind and severe convection first appear in the Bay of Bengal and then gradually spread eastward to the region of South China Sea. The Bay of Bengal is the region that has the earliest outbreak of the Southwest Monsoon in Asia as a whole. The southwest monsoon sets up earlier in the northern than in the southern part of the SCS.

1998 is the weak monsoon year and the OLR and southwesterly wind are respectively about 1 month and 1/2 month in oscillatory cycles. The monsoon in the Bay of Bengal and the cross-equatorial airflows are two important driving sources for the low-frequency oscillations of the SCS monsoon.

There is a significant relation of interactions between the SCS southwest monsoon and the SST in the Pacific Ocean ~ Indian Ocean. That a strong warm water episode exists in early spring 1998 for the equatorial eastern Pacific accounts for much of the reason why the SCS region is in a year of weak summer monsoon and why the SCS monsoon dominates in the interactions of SST between the South China Sea and the Arabian Sea, leading to higher SST.

Acknowledgements: It is much appreciated that Mr. CAO Chao-xiong, who works at the Guangzhou Institute of Tropical and Oceanic Meteorology, has translated our paper into English.

REFERENCES:

- CHEN Long-xun, SONG Yi, Murakami M, 1996. Variations of convective cloud clusters during the onset period of summer monsoon [A]. *In: Latest Advances in the study of East Asian Monsoon*, edited by HE Jin-hai et al. [C]. Beijing: China Meteorological Press, 54-65.
- DING Yi-hui, MA He-nian, 1996. The state-of-the-art of research on East Asian monsoon [A]. *In: Latest Advances in the study of East Asian Monsoon*, edited by HE Jin-hai et al. [C]. Beijing: China Meteorological Press, 1-16.
- HE Jin-hai, LUO Jing-jia, 1996. Outbreaks of South China Sea monsoon and advancement of Asian summer monsoon and discussions of formation mechanism [A]. *In: Latest Advances in the study of East Asian Monsoon*, edited by HE Jin-hai et al. [C]. Beijing: China Meteorological Press, 74-81.
- LAU K-M, SONG Yang, 1997. Climatology and interannual variability of the Southeast Asian summer monsoon [J]. *Adv. Atmos. Sci.*, **14**: 141-162.
- LI Cheng-feng, MICHIO Y, 1996. The onset and interannual variability of the Asia summer monsoon in relation to land-sea thermal contrast [J]. *J. Climate*, **9**: 358-375.
- LIANG Jian-yin, WU Shang-sen, YOU Ji-ping, 1999. The research on variations of onset time of the SCS summer

- monsoon and its intensity [J]. *J. Trop. Meteor.*(Chinese Ed.), **15**(2): 97-105.
- LIU Xia, XIE An, YE Qian et al., 1998. The climatic characteristics of summer monsoon onset over South China Sea [J]. *J. Trop. Meteor.*(Chinese Ed.), **14**(1): 28-37.
- WANG Qi-yi, DING Yi-hui, 1997. Climatological aspects of evolution of summer monsoon over the northern South China Sea [J]. *Acta Meteor. Sin.*, **55**(4): 466-483.
- WEBSTER P J, YANG S, 1992. Monsoon and ENSO: Selectively interactive systems [J]. *Quart. J. Roy. Meteor. Soc.*, **118**: 877-926.
- WU Guo-xiong, MENG Wen, 1998. Gearing between the Indo-monsoon circulation and the Pacific-Walker circulation and the ENSO. Part I: Data analyses [J]. *Sci. Atmos. Sin.*, **22**(4): 470-480.
- WU Shang-sen, LIANG Jian-yin, 1998. Seasonal evolution of climatic characteristics of summer monsoon over Xisha area. [J] *Sci. Atmos. Sin.*, **22**(5): 771-778.
- YAN Jun-yue, 1997. Climatological characteristics on the onset of the South China Sea southwest monsoon [J]. *Acta Meteor. Sin.*, **55**(2): 174-186.